Predictive design and layer-by-layer characterization of 3D-printed multi-layer micro-perforated panels for broadband sound absorption

D.Soumah, N. M. Murad, A.F. Rabearivony, S. G. Menard
PIMENT Laboratory, University of La Réunion, France
P. Andriniriniaimalaza
ISSTM, University of Mahajanga, Madagascar
A. Georgiev
University of Telecommunications and Posts, Sofia, Bulgaria

Introduction

Environmental noise pollution is a major public health issue, particularly in tropical island environments such as La Réunion, where noise is compounded by humidity constraints that degrade conventional fibrous and porous absorbers over time. Long-term exposure contributes to sleep disturbance, cognitive impairment and cardiovascular diseases [1]. Conventional sound-absorbing materials such as mineral wool or fiberglass require significant thickness to be effective at low frequencies and are particularly unsuitable for tropical climates due to moisture-induced degradation [2-3].

Micro-Perforated Panels (MPPs) offer a promising sustainable alternative: lightweight, tunable broadband absorbers requiring no fibrous filling, fabricable from recyclable thermoplastics via FDM 3D printing. A Transfer Matrix Method (TMM) simulator was developed in Python to predict α(f) and Z(f) of multi-layer configurations. This work presents the design, simulation and experimental characterization of multi-layer FDM-printed MPP absorbers, and proposes a calibration methodology to bridge the gap between TMM predictions and measurements.

THEORETICAL BACKGROUND

A micro-perforated panel absorber (MPPA) consists of a thin panel of thickness t, perforated with holes of diameter d, placed before a rigid-backed air cavity of depth D [4-5]. At normal incidence, the normalized surface impedance is:

$$Z_1 = Z_{MPP} + Z_D$$

where Z_MPP is the panel impedance and Z_D = −jZ₀cot(ωD/c₀) is the cavity impedance. The normal-incidence absorption coefficient is:

$$\alpha = 1 - \left|\frac{Z_1 - 1}{Z_1 + 1}\right|^2$$

Maximum absorption (α → 1) occurs at resonance frequency:

$$f_0 \approx \frac{c_0}{2\pi}\sqrt{\frac{\phi}{L_{\text{eff}} D}}$$

where c₀ is the speed of sound, φ the perforation ratio, and L_eff = t + δ the effective perforation length including the end-correction δ accounting for air mass radiation at hole openings.

Experimental setup

Measurements were performed in a circular impedance tube (Ø 40 mm) using the transfer function method (ISO 10534-2) [6] over 50–4500 Hz at ~23°C. Three three-layer MPP assemblies (Fig 1-3) were tested, sharing identical cavity depths (D = 20 mm) and hexagonal perforation pattern but differing in hole diameter d and centre-to-centre spacing a. A solid PLA cylinder confirmed quasi-rigid backing behaviour (α < 0.21 across the full range), validating the rigid termination assumption of the TMM.

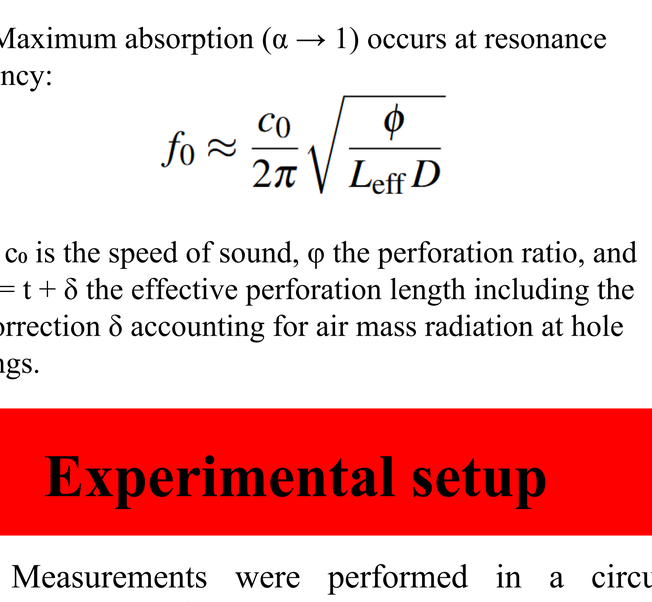

Fig. 1. Multi-layer MPP specimens: CAD design

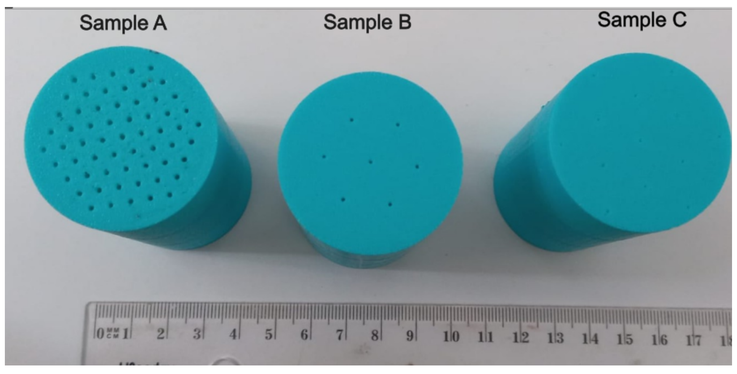

Fig. 2. Multi-layer MPP specimens: FDM-printed PLA samples (sample A to C from left to right).

Tab. 1. Summary of fabricated specimens and key geometric parameters. d: hole diameter; a: distance between the center of two holes; t: panel thickness; φ : perforation ratio; D: cavity depth; n: number of holes.

Samples	Config.	d (mm)	a (mm)	t (mm)	ϕ (%)	D (mm)	n
Sample A	Layer 1	1.60	4	2	9.91	20	61
	Layer 2	1.60	4	3	9.91	20	61
	Layer 3	1.60	4	3	9.91	20	61
Sample B	Layer 1	1.20	10	2	0.68	20	7
	Layer 2	1.20	10	3	0.68	20	7
	Layer 3	1.20	10	3	0.68	20	7
Sample C	Layer 1	1	10	2	0.83	20	13
	Layer 2	1	10	3	0.83	20	13
	Layer 3	1	10	3	0.83	20	13

Results

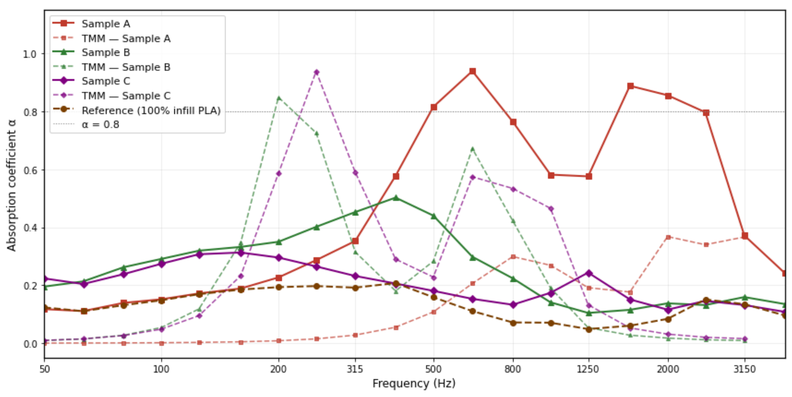

Fig. 3. Measured absorption coefficient (third-octave bands) for samples A, B and C and the PLA reference cylinder. TMM predictions (dashed lines) are shown for each sample

Sample A achieves α > 0.8 in two frequency bands: 500–630 Hz (α_max = 0.94) and 1600–2000 Hz. The TMM significantly underestimates absorption (α_max ≈ 0.4), attributable to FDM wall roughness increasing viscous resistance by a factor of 10–15.

Sample B shows a moderate peak (α_max = 0.50 at 400 Hz). The TMM overestimates, predicting α ≈ 0.93 at 250 Hz.

Sample C exhibits a flat, featureless curve (α_max = 0.31), FDM surface irregularities fully suppress the Helmholtz resonance mechanism at this hole diameter.

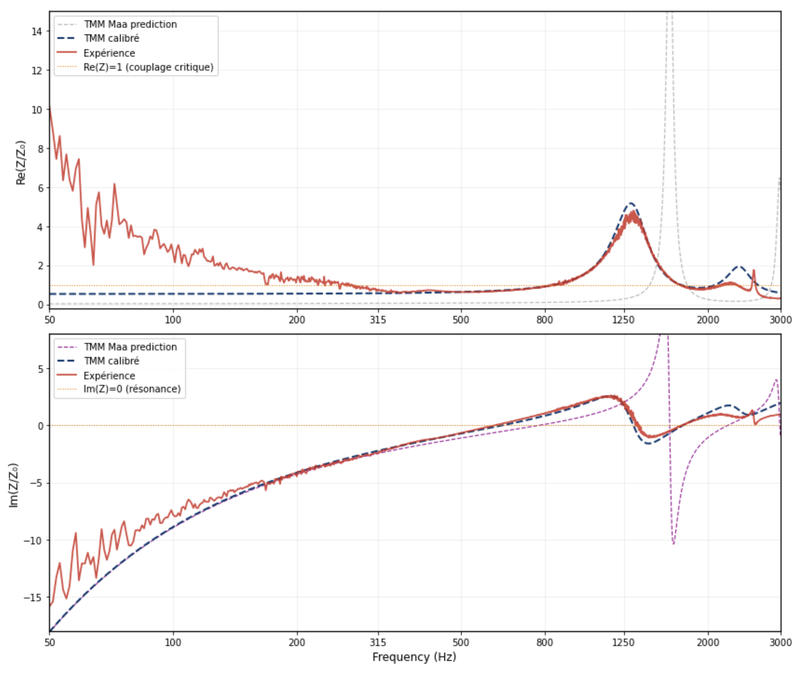

Fig. 4. Normalized impedance Z(f) of sample A: real part Re(Z) (top) and imaginary part Im(Z) (bottom). TMM nominal (purple), experiment (red) and calibrated TMM (blue)

Impedance analysis of Sample A reveals that Im(Z) is well predicted up to 1300 Hz, while Re(Z) is underestimated by a factor of 10–15. A resonance frequency shift of 21.8% (774 Hz predicted vs. 605 Hz measured) indicates that the effective end-correction significantly exceeds the Fok prediction.

An empirical calibration using a rugosity factor ξ_r and end-correction factor ξ_δ substantially reduces the RMSE for Sample A (Re(Z): 3.13 → 0.72; Im(Z): 3.00 → 0.57) but fails for Sample C, revealing a fundamental acoustic regime change at small hole diameters.

Tab. 2. Calibration results. RMSE computed over 50–3000 Hz on normalized Re(Z) and Im(Z).

Samples	Calib.	ξ_r	ξ_δ	R_0	RMSE Re(Z)	RMSE Im(Z)
Sample A	Pur Maa	1	1	1	3.13	3.0
	Calib.(auto)	5.14	3.80	0	0.72	0.57
Sample B	Pur Maa	1	1	1	3.54	3.80
	Calib.(auto)	2.37	0.8	0	2.00	2.99
Sample C	Pur Maa	1	1	1	3.51	7.50
	Calib.(auto)	0.5	5	0	3.66	8.56

These findings establish a clear hierarchy of FDM-induced effects: wall roughness dominates the resistive component Re(Z), while the reactive component Im(Z) remains well captured by the smooth-wall Maa model up to 1300 Hz. This separation is practically valuable, it means TMM can still reliably guide resonance frequency tuning through cavity depth D and perforation ratio φ, while absorption amplitude requires a single empirical Re(Z) measurement for calibration.

Conclusions

Multi-layer FDM-printed MPP absorbers demonstrate strong broadband absorption potential: Sample A achieves α_max = 0.94, significantly exceeding TMM predictions. Impedance analysis identifies FDM wall roughness as the dominant factor inflating Re(Z), while Im(Z) remains well captured by the Maa model up to 1300 Hz. This separation provides a practical diagnostic framework: TMM retains validity for resonance frequency tuning via D and φ, but requires empirical Re(Z) calibration for accurate amplitude prediction. Future work will target frequency-specific multi-layer configurations and systematic characterization of printing parameter effects on Z^eff_MPP, toward reliable predictive design of sustainable FDM-printed acoustic metamaterials.

These results confirm that FDM printing introduces systematic deviations from classical MPP theory, primarily through wall roughness and dimensional shrinkage [7], but does not fundamentally prevent the design of efficient broadband absorbers. The proposed calibration framework provides a practical route toward reliable predictive design, paving the way for sustainable, low-cost acoustic treatments adapted to tropical environments.

References

[1] M. S. Razai et al. "The impact of noise pollution on health". BMJ 391, e081193 (2025).

[2] A. Rabearivony and N. Murad. "Sustainable acoustic metamaterials from recycled plastic bottles." Sustainable Materials and Technologies 48, e01939 (2026).

[3] M. Mohammadi et al. "A Comprehensive Review of Factors Influencing the Sound Absorption Properties of MPP Structures." J. Vibration Engineering & Technologies 13.5, p. 319 (2025).

[4] D.-Y. Maa. "Potential of microperforated panel absorber." J. Acoustical Society of America 104 (1998).

[5] P. Cobo. "Modelling of Microperforated Panel Absorbers with Circular and Slit Hole Geometries." Acoustics 3.4, pp. 665–678 (2021).

[6] AFNOR. Acoustique — Détermination des propriétés acoustiques aux tubes d'impédance, Partie 2 : méthode à deux microphones. ISO 10534-2 (2023).

[7] Deepak et al. "Exploring the acoustic potential of 3D printed micro-perforated panels: A comparative analysis." Heliyon 10.7, e28612 (2024).